Identification of 6-benzyloxysalicylates as a novel class of inhibitors of 15-lipoxygenase-1

Eleftheriadis, Nikolaos; Thee, Stephanie; Te Biesebeek, Johan; van der Wouden, Petra; Baas, Bert-Jan; Dekker, Frank J

Published in:
European Journal of Medicinal Chemistry

DOI:
10.1016/j.ejmech.2015.03.007

Publication date:
2015

European Journal of Medicinal Chemistry 94 (2015) 265–275

Contents lists available at ScienceDirect

European Journal of Medicinal Chemistry

journal homepage: http://www.elsevier.com/locate/ejmech

Original article

Identification of 6-benzyloxysalicylates as a novel class of inhibitors of 15-lipoxygenase-1

Nikolaos Eleftheriadis [a], Stephanie Thee [a], Johan te Biesebeek [a], Petra van der Wouden [a], Bert-Jan Baas [b], Frank J. Dekker [a, *]

[a] Department of Pharmaceutical Gene Modulation, Groningen Research Institute of Pharmacy, University of Groningen, Antonius Deusinglaan 1, 9713 AV Groningen, The Netherlands
[b] Department of Pharmaceutical Biology, Groningen Research Institute of Pharmacy, University of Groningen, Antonius Deusinglaan 1, 9713 AV Groningen, The Netherlands

ARTICLE INFO

Article history:
Received 14 November 2014
Received in revised form
2 March 2015
Accepted 3 March 2015
Available online 5 March 2015

Keywords:
Lipoxygenase
Expression
Inhibitor
Enzyme kinetics
Salicylate

ABSTRACT

Lipoxygenases metabolize polyunsaturated fatty acids into signalling molecules such as leukotrienes and lipoxins. 15-lipoxygenase-1 (15-LOX-1) is an important mammalian lipoxygenase and plays a crucial regulatory role in several respiratory diseases such as asthma, COPD and chronic bronchitis. Novel potent and selective inhibitors of 15-LOX-1 are required to explore the role of this enzyme in drug discovery. In this study we describe structure activity relationships for 6-benzyloxysalicylates as inhibitors of human 15-LOX-1. Kinetic analysis suggests competitive inhibition and the binding model of these compounds can be rationalized using molecular modelling studies. The most potent derivative **37a** shows a K_i value of 1.7 μM. These structure activity relationships provide a basis to design improved inhibitors and to explore 15-LOX-1 as a drug target.

1. Introduction

Lipoxygenases (LOXs) are non-heme, iron containing enzymes which can be found in both plant and animal kingdoms. Located in the cytosol or other organelles [1], lipoxygenases catalyse the regio- and stereospecific insertion of oxygen (O_2) into polyunsaturated fatty acids (PUFAs), such as arachidonic or linoleic acid, which contain a series of *cis* double bonds [2]. These molecules are essential fatty acids in humans and are formed from membrane lipids that are hydrolysed by cytosolic phospholipase A2 (cPLA2) [3]. These conversions result in hydroperoxy fatty acids, or eicosanoids, that are further metabolized into signalling compounds such as leukotrienes and lipoxins [4–8], which play a regulatory role in several inflammatory and respiratory diseases. Mammalian lipoxygenases are denoted 5-, 8-, 12- and 15-LOX based on the site of oxygenation of arachidonic acid [2]. Human 15-LOX appears in two isoforms h-15-LOX-1 and h-15-LOX-2 [9]. This study aims at identification of new types of inhibitors to explore h-15-LOX-1 as a potential therapeutic target.

Arachidonic acid and linoleic acid can both act as substrates of 15-LOX-1, however linoleic acid seems to be the preferred substrate by this enzyme [10–12]. Interestingly, this lipid is the major polyunsaturated fatty acid in human nutrition and diet [13,14]. This is quite remarkable since arachidonic acid is the major substrate for most other mammalian lipoxygenases. 15-LOX-1 has a molecular mass of 74.804 Da and consists of 662 amino acids. Both isoforms of human 15-LOX are predominantly expressed in airway epithelial cells, reticulocytes, eosinophils, alveolar macrophages, mast cells and dendritic cells [10,15–21]. Certain interleukins have been shown to induce the expression of 15-LOX in cultured mast cells, monocytes and epithelial cells [21–23]. These findings suggest that these cytokines may act as important physiological and pathophysiological regulators of 15-LOX *in vivo* [16]. Being expressed in many immune cells found in the respiratory tract and in the skin, these enzymes have been implicated in several immune diseases.

When arachidonic acid becomes available, 15-LOX converts this polyunsaturated fatty acid into 15S-hydroperoxy-5*Z*,8*Z*,11*Z*,13*E*-eicosatetraenoic acid (15(S)-HPETE). This compound can be reduced to 15(S)-HETE [19,24–26] and eventually to 15-oxo-5*Z*,8*Z*,11*Z*,13*E*-eicosatetraenoic acid (15-OxoETE) [27]. Some studies suggest that these molecules are involved in cancer. For example,

* Corresponding author.
E-mail address: f.j.dekker@rug.nl (F.J. Dekker).

http://dx.doi.org/10.1016/j.ejmech.2015.03.007
0223-5234/

15(S)-HPETE and 15(S)-HETE have shown to inhibit chronic myeloid leukaemia cells by inducing apoptosis [28]. Therefore, it is suggested that 15-LOX might have anti-carcinogenic effects. 15(S)-HPETE is also metabolized into lipoxins or eoxins. 5-LOX is able to convert 15(S)-HPETE to 5S,6S,15S-epoxytetraene, which then can be further metabolized in lipoxins A4 (LXA4), lipoxins B4 (LXB4) and Lipoxin C4 (LXC4) by LXA4 hydrolase, LXB4 hydrolase and GSH-transferase respectively. Lipoxin D4 (LXD4) and lipoxin E4 (LXD4) are produced from LXC4 by γ-glutamyl transferase and dipeptidase respectively. In addition to lipoxins also eoxins (also referred as 14,15-leukotrienes [16]), can be produced by conversion of 15(S)-HPETE by 15-LOX itself to eoxin A4 (EXA4) [15,16,24,25]. To produce the other eoxins EXC4, EXD4 and EXE4, a chain reaction with EXA4 as the starting molecule occurs [15,16,29]. While lipoxins are anti-inflammatory, eoxins have shown to be pro-inflammatory mediators. Having similar actions as leukotrienes, they may be implicated in several respiratory diseases such as asthma, COPD and chronic bronchitis. In addition, they may play a role in atherosclerosis, rhinitis and in certain types of cancer like Hodgkin's disease [15,16,29]. In conclusion, 15-LOX is responsible for the biosynthesis of lipoxins and eoxins which are anti-inflammatory and pro-inflammatory mediators, respectively. Application of small molecule inhibitors of 15-LOX in disease models is the next step towards defining the role of 15-LOX as a potential therapeutic target in inflammatory diseases.

Due to the key role of 15-LOX-1 in several disease processes, small molecule inhibitors of this enzyme have been developed. One of these inhibitors is PD-146176, reported by Parke-Davis (now Pfizer) [30]. Other researchers from Bristol-Myers Squibb (BMS) identified tryptamine-based compounds [31], imidazole-based compounds [32] and pyrazole-based compounds [33] as inhibitors for 15-LOX with low nanomolar affinity. However, since these compounds have unfavourable physical properties, it is unlikely that they would continue for the development as drugs [34]. In addition, 3-aroyl-1-(4-sulfamoylphenyl)thiourea [35] and pyrimidinylthio-pyrimidotriazolothiadiazines [36] derivatives were published as 15-LOX inhibitors. These compounds have shown to have affinities against soybean 15-LOX with ranging IC_{50} values of 2–25 μM.

Inspired by our previous identification of a 6-benzyloxysalicylate as an allosteric activator of h-5-LOX [37], we now present 6-benzyloxysalicylates as a new class of compounds for competitive inhibition of h-15-LOX-1. A focused compound collection of 6-benzyloxysalicylate and benzyloxyphenyl derivatives was synthesized and screened for inhibition of h-15-LOX-1 to derive structure activity relationships. The results were rationalized using molecular modelling studies.

2. Results and discussion

2.1. Synthesis

A compound collection was designed based on previously published salicylates **8b-c** that were reported as modulators for human 5-lipoxygenase activity [37,38]. In this study, we expanded the compound collection by the synthesis of compounds that consist of three parts, A, B and C (Table 1, Fig. 1). For the A part, different substituted aromatic moieties were used, which include hydrogen bond donors or acceptors or halides. The B part was kept constant and for the C part, four aliphatic chains with a different number of carbons were used to explore hydrophobic interactions.

The *p*-alkyloxybenzylbromides **4a-d** were prepared in three steps starting from *p*-hydroxybenzaldehyde (Scheme 1). Alkylbromides were coupled with *p*-hydroxybenzaldehyde using the Williamson ether synthesis to give the corresponding benzaldehyde ethers **2a-d**. Subsequently, benzaldehydes were reduced to benzyl alcohols **3a-d** using sodium borohydride in high yields. The *p*-alkyloxybenzylbromides **4a-d** were obtained after the bromination of the benzyl alcohols **3a-d** using PBr_3 as a reagent in high yields. The three salicylate final products **8a-d** were prepared in three reaction steps. Firstly, 2,6-dihydroxybenzoic acid **5** was converted to acetonide **6** as previously described by Uchiyama et al. [37,39,40]. Secondly, acetonide **6** and the *p*-alkyloxybenzylbromides **4a-c** were coupled via the Williamson ether synthesis to the corresponding ethers **7a-c**. Finally, the final products **8a-c** were obtained after the deprotection of the acetonide group using potassium hydroxide in THF in good yields. In order to avoid degradation of the salicylate products **8a-c**, the products were not acidified in the last step. Instead the final products were isolated as potassium salts. The compounds **17–28** were prepared by the direct coupling of the substituted phenols **9–16** and the *p*-alkyloxybenzylbromides **4a-d** in good yields.

The enantiomerically pure products **37a,b** were prepared in eight reaction steps starting from commercially available (R)-(+)- or (S)-(−)-Citronellal (Scheme 2). As a first step the aldehydes **30a,b** were reduced to alcohols **31a,b** using sodium borohydride and the double bonds were reduced with Pd/C under H_2 atmosphere to give **32a,b**. The alcohols were brominated using tetrabromomethane to give **33a,b**. Bromides **33a,b** were coupled to *p*-hydroxybenzaldehyde using the Williamson ether synthesis to give the ethers and after reduction of the aldehydes the corresponding alcohols **34a,b** were obtained in high yields. **34a,b** were converted into the bromides **35a,b** by bromination of the corresponding alcohols. After the coupling between the bromides **35a,b** and acetonide **6** and the deprotection using potassium hydroxide in THF in good yields the final compounds **37a,b** were isolated as potassium salts.

2.2. Enzyme inhibition

Recombinant h-15-LOX-1 was expressed in *E. coli* BL21(DE3) containing a pET26 h-15-LOX-1 expression plasmid [41]. The enzyme was purified by gravity flow on a Ni-sepharose column. h-15-LOX-1 activity was determined by the conversion of linoleic acid to 13S-hydroperoxy-9Z,11*E*-octadecadienoic acid (13(S)-HpODE). The conversion rate was followed for by UV-absorbance at 234 nm over time. We observed, however, that the stability of the purified h-15-LOX-1 was relatively poor and the enzyme loses its activity after four days storage at −80 °C. Nevertheless, the crude bacterial lysate containing the expressed enzyme provides enzyme activity after prolonged storage at −80 °C (6 months) (Fig. S2). Control experiments were performed to test if the observed activity could be assigned to the expressed h-15-LOX-1 and not to other proteins present in the crude bacterial lysates. Towards this aim the lysates of bacteria without the h-15-LOX-1 expression plasmid gene were tested in the same dilution for their ability to convert linoleic acid in this assay. In these tests no background activity has been observed (Fig. S3).

Using the crude bacterial lysates with overexpressed h-15-LOX-1 a collection of previously published [37,38] and newly synthesized products were screened for inhibition at concentrations of 50 μM. The residual enzyme activity was measured after 10 min pre-incubation with the inhibitors at room temperature. Aside from the newly synthesized compounds, the known inhibitors, **PD-146176** (15-LOX) and **Zileuton** (5-LOX), were also tested. The results of the screening are shown in Fig. 2.

The inhibition of h-15-LOX-1 for the compounds with the salicylate functionality were 70% for **8a** (PK147), 50% for **8b** (N195) and no inhibition for **8c-d**. This indicates that the aliphatic tail in the C part should be larger than 5 carbon atoms and branching of

Table 1
Compound collection.

Compounds		R^1	R^2	R^3	R^4
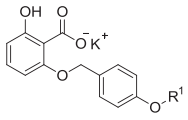	**8a** (PK147)	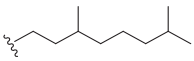	–	–	–
	8b (N194)	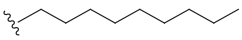			
	8c (PK131)	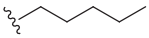	–	–	–
	8d (TBK10)		–	–	–
	37a (N206)	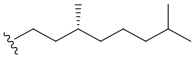	–	–	–
	37b (N219)	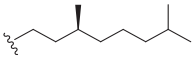	–	–	–
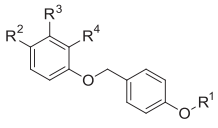	**17** (TBK25)	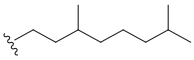	Cl	H	H
	18 (N78)		H	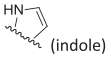 (indole)	
	19 (N193)			H	H
	20 (TBK29)		Cl	H	H
	21 (B10)			H	H
	22 (B11)		H	NO_2	H
	23 (TBK33)	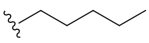	Cl	H	H
	24 (TBK47)		I	H	H
	25 (TBK48)		 (naphthyl)		H
	26 (TBK55)		CHO	H	H
	27 (TBK57)		H	H	CHO
	28 (B5)	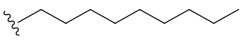		H	H
	29 (B6)		H	NO_2	H

the aliphatic tail improves the activity. Furthermore, for the compounds in which the salicylate functionality (part A) is replaced for other aromatic functionalities little inhibition is observed (**18** (N78), **28** (B5) and **29** (B6)). Considering these data the most potent inhibitor **8a** (PK147) and the known 15-LOX-1 inhibitor **PD-146176** were subjected to IC_{50} determination, which proved to be 10 ± 1 μM for **8a** (PK147) and 16 ± 2 μM for **PD-146176** (Fig. S4). In literature, **PD-146176** is described as a selective non-competitive inhibitor for 15-LOX with reported IC_{50} values of 0.54 μM [42], 1.1 μM [43] and 3.8 μM [44]. These values cover the same concentration range and the differences are most likely due to differences in the applied substrate concentrations in the assays. Taking this together we conclude that we identified **8a** (PK147) as a hit with comparable potency as the known inhibitor **PD-146176**. Interestingly, **8a** (PK147) has been subjected to inhibition studies on h-5-LOX and COX-2 in a previous study [37]. It inhibits h-15-LOX-1 with 80%, h-5-LOXs with 50%, and COX-2 with 30% at 50 μM, which indicates a certain level of selectivity for h-15-LOX-1 inhibition (Fig. S5). Both enantiomers of **8a** (PK147) were synthesized and their inhibitory potencies were investigated. The (R)-(+) enantiomer **37a** (N206) showed an IC_{50} of 7.1 μM and the S-(−) enantiomer **37b** (N219) showed an IC_{50} of 42 μM, which indicates a 6-fold difference in potency between both enantiomers (Table 1 and Fig. 3).

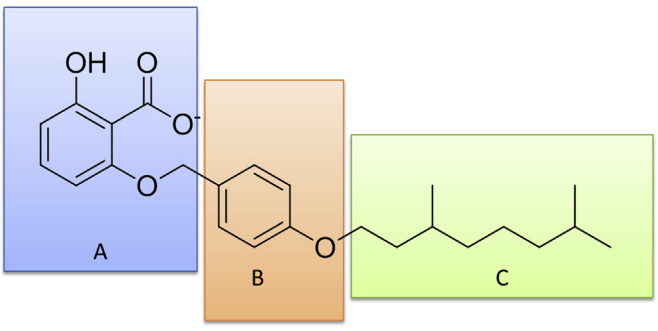

Fig. 1. General structure of the synthesized compounds in which parts A, B and C were varied.

2.3. Enzyme kinetic studies

After having identified the most potent inhibitors in this compound collection we moved on to enzyme kinetic analysis. The enzyme kinetics of h-15-LOX-1 using linoleic acid as a substrate revealed substrate inhibition at concentrations above 60 μM (Fig. 4A). Therefore, the analysis was done with substrate concentrations below 60 μM for enzyme kinetic studies. In order to establish the mechanism of h-15-LOX-1 inhibition, enzyme kinetic analysis in presence of inhibitor **8a** was performed (Fig. 4B). Inhibitor **8a** causes an increase in K_m compared to the control whereas the V_{max} remains more constant compared to the control (Table 3), which indicates competitive inhibition. Using the Cheng-

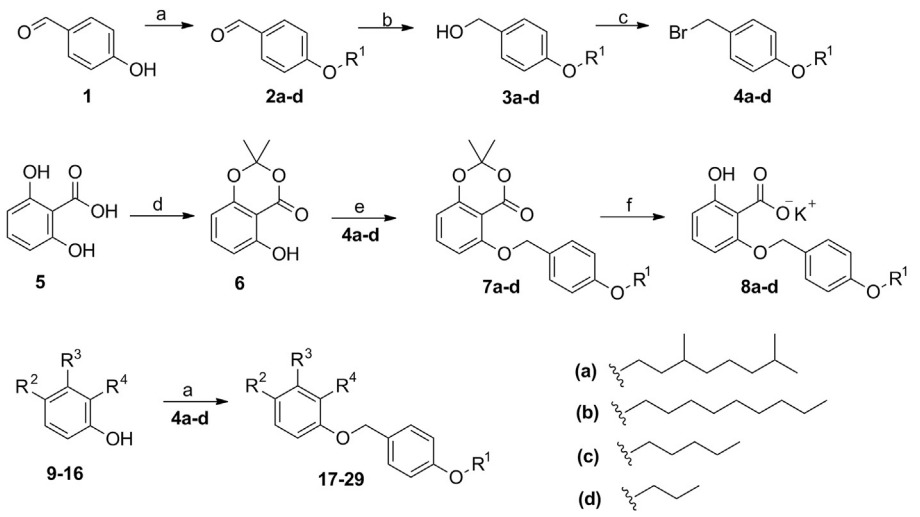

Scheme 1. Reagents and conditions: a) 1-bromo alkane, K_2CO_3, DMF, R.T. overnight; b) $NaBH_4$, MeOH, R.T. for 1 h; c) PBr_3, CH_2Cl_2, 0 °C for 2 h; d) $SOCl_2$, DMAP, DME, Acetone, 0 °C for 1 h, then R.T. overnight ;e) compounds **4a**–**d**, K_2CO_3, DMF, R.T. overnight; f) 5 M KOH, THF, 60 °C overnight.

Prusoff equation the binding affinity (K_i) of the inhibitor **8a** was calculated to be 2.4 μM and for the inhibitor **37a** 1.7 μM. For comparison we previously reported a K_i for h-5-LOX of 70 μM for **8a** [37], which indicates a more then 10-fold affinity difference between h-5-LOX and h-15-LOX-1 inhibition. The K_i value for the inhibitor **PD-146176** was calculated to be 3.9 μM (Table 2) which is in line with previous mentioned literature.

2.4. Molecular modelling

A docking study was performed in order to gain insight in the mode of binding of these compounds. Because there is no crystal structure of human 15-LOX available the study was performed with the crystal structure of rabbit 15-LOX as determined by Gillmor et al. [45] This is justified by the high sequence similarity (87%) between rabbit 15-LOX and human 15-LOX-1 (Fig. S6). Since competitive inhibition was observed both enantiomers **37a** and **37b** were docked in the active site of the enzyme. In the highest scoring docking poses, the inhibitor **37a** forms a hydrogen bond between the salicylate carbonyl and the amino acid Arg403 (Fig. 5A). In addition, the methyl group of the branched lipid chain of **37a** is involved in an arene–hydrogen interaction with His361. The lipid chain seems to occupy the entire space in the substrate binding pocket (Fig. 5B). Docking of the S-enantiomer **37b** demonstrates a mismatch of the aliphatic tail with the substrate binding pocket resulting the absence of the arene–hydrogen interaction with His361, which is in line with the observed 6-fold difference between both enantiomers (Fig. S8).

The other salicylate inhibitors with shorter and non-branched aliphatic tails were docked in the same way and the docking poses with the highest scoring bind similarly in the active site. However, it seems that they cannot bind the enzyme as well as the compound **37a** because of a mismatch in the hydrophobic pocket. In case of the compounds **8d** and **8c**, the aliphatic chain is too short and in case of the compound **8b** the chain is long enough but not branched to fill the entire pocket thus providing less activity than **37a**. The good fit of **37a** in the binding pocket is reflected in its relatively high docking score compared to the other investigated compounds with weak of no inhibition for h-15-LOX-1 (Table 4).

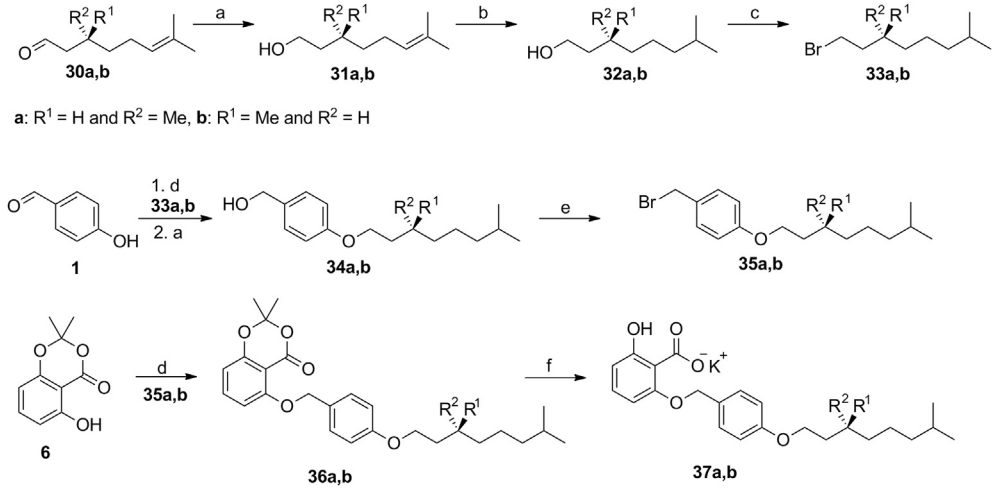

Scheme 2. Reagents and conditions: a) $NaBH_4$, MeOH, R.T. for 1 h; b) H_2, Pd/C, EtOH, R.T. overnight; c) CBr_4, PPh_3, CH_2Cl_2, 0 °C for 3 h; d) K_2CO_3, DMF, R.T. overnight; e) PBr_3, CH_2Cl_2, 0 °C for 2 h; f) 5 M KOH, THF, 60 °C overnight.

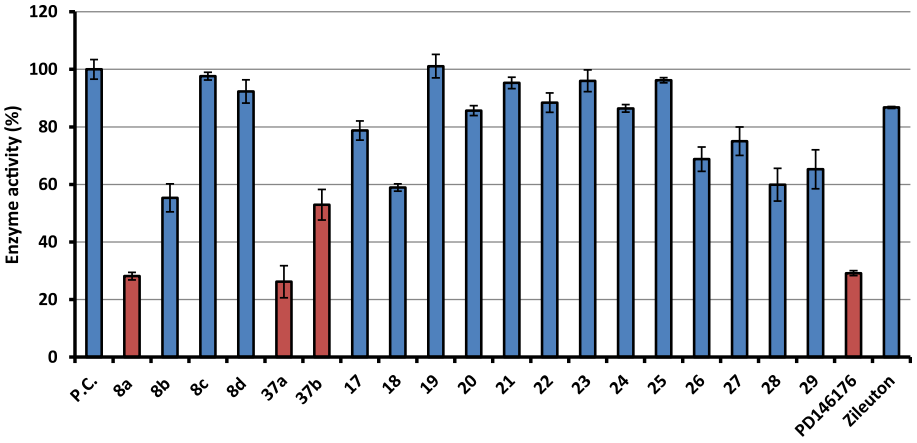

Fig. 2. Residual enzyme activity that was observed for the screening of a compounds collection for inhibition of h-15-LOX-1 in presence of 50 μM of the respective compounds (Table 1). The enzyme activity in absence of inhibitor was set to 100% and the background signal in absence of the overexpressed h-15-LOX-1 was set to 0%. The averages and standard deviations of the individual measurements are shown.

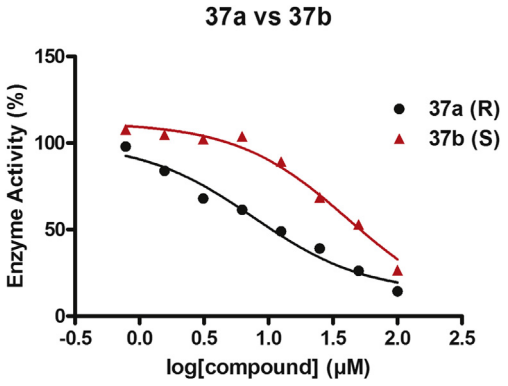

Fig. 3. IC_{50} plots of h-15-LOX-1 inhibition with **37a** (N206) and **37b** (N219). The results are averages of triplicates and the curves are derived by non-linear curve fitting. All the values are reported with the standard deviation after non-linear curve fitting. After t-test, the p-value (0.009) showed significant difference between the IC_{50} values of compounds **37a** and **37b**.

2.5. Additional studies

Focussing on compound **37a** with the highest affinity, ligand efficiency metrics were calculated (Table 5). Ligand efficiency is defined as the binding affinity of a ligand in relation to the number of non-hydrogen atoms (HA) according the Equation LE = (1.37/HA) × pKi [46]. Compound **37a** has 29 heavy atoms (non-hydrogen) and the K_i value is 1.7 μM, which gives an LE equal to 0.27 Kcal per mol per heavy atom. This value is close to the proposed acceptable values of LE for drug candidates, which should be >0.3 Kcal per mol per heavy atom. Furthermore, the binding efficiency index (BEI) and the surface efficiency index (SEI) were calculated according to Equations BEI = pKi/MW and SEI = pKi/(PSA/100 $Å^2$). BEI is the binding efficiency index relating potency to molecular weight on a per kDa scale and SEI is the surface efficiency index monitoring the potency gains as related to the increase in polar surface area (PSA) referred to 100 $Å^2$ [47]. The MW of the compound **37a** is 399 Da or 0.399 KDa, so the BEI is 14.46. The Polar surface area (PSA) was estimated from ChemDraw 12.0 software to 78.82 and according to that the SEI is equal to 7.31. Mapping of the surface-binding and binding efficiency indices (SEI–BEI values) for the 92 examples of marketed drugs showed average SEI of 14.5 ± 8.7 and BEI of 25.8 ± 7.9 [48]. Therefore, according to the ligand efficiency metrics, compound **37a** approaches the requirements as a candidate drug. All the ligand efficiency metrics were presented at Table 5.

3. Conclusions

In this study, we describe the synthesis and the characterization of 6-benzyloxysalicylates as a new class of inhibitors of h-15-LOX-1. Enzyme inhibition and kinetic studies as well as molecular modelling studies has been performed in order to characterize a structurally novel inhibitor **37a** (N206), which proved to be a competitive inhibitor of h-15-LOX-1 with a K_i value of 1.7 μM. Compound **37a** is the R enantiomer of the racemic mixture **8a**, while the S enantiomer, compound **37b** is 6-fold less active. Molecular modelling studies indicate that compound **37a** occupies

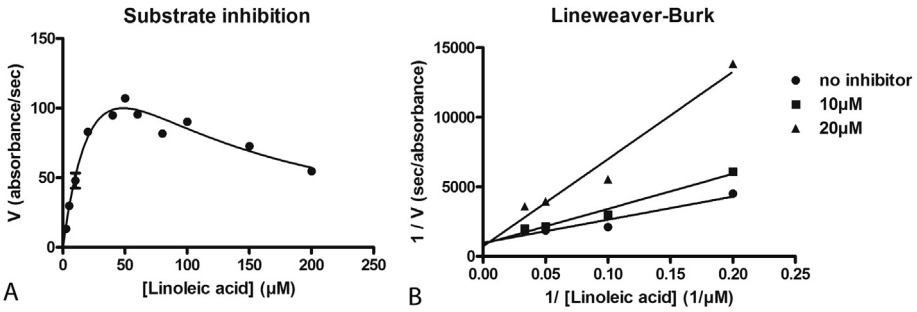

Fig. 4. A) Substrate inhibition plot of linoleic acid conversion by h-15-LOX-1, B) Steady-State kinetic characterization of h-15-LOX-1 in presence of different concentrations of inhibitor **8a** (PK147).

Table 2
IC_{50} and K_i values of the inhibitors for inhibition of h-15-LOX-1.

Compound	IC_{50} (μM)	K_i (μM)
PD-146176	16 ± 2.5	3.9 ± 0.6
8a (PK147)	10 ± 1.3	2.4 ± 0.4
37a (N206)	7.1 ± 4.6	1.7 ± 1.1
37b (N219)	42 ± 12	10 ± 3.0

most of the available space in the substrate binding pocket while the S-enantiomer **37b** demonstrates a mismatch of the aliphatic tail with the substrate binding pocket. In the future, these inhibitors could be employed as starting point for drug discovery effort aimed at h-15-LOX-1 and in pharmacological studies on the utility of this enzyme as a drug target.

4. Experimental section

4.1. Synthesis and characterization

4.1.1. General

The solvents and reagents were purchased from Sigma–Aldrich and Acros chemicals and were used without further purification. Reactions were monitored by thin layer chromatography (TLC). Merck silica gel 60 F_{254} plates were used and spots were detected with UV light. MP Ecochrom silica 32-63, 60 Å was used for flash column chromatography. ^1H NMR (500 MHz) and ^{13}C (126 MHz) spectra were recorded with a Bruker Avance 4-channel NMR Spectrometer with TXI probe. Chemical shifts are reported in ppm relative to the solvent. Atmospheric Pressure Photoionization mass spectra (APPI-MS) were recorded on an Applied Biosystems/SCIEX API3000-triple quadrupole mass spectrometer and electrospray ionization mass spectra (ESI-MS) were recorded on a Waters Investigator Semi-prep 15 SFC-MS instrument.

The compounds **8a**, **8c**, **8b**, (4-(pentyloxy)phenyl)methanol, 1-(bromomethyl)-4-(pentyloxy)benzene, (4-((3,7-dimethyloctyl) oxy)phenyl)methanol, 1-(bromomethyl)-4-((3,7-dimethyloctyl) oxy)benzene, (4-(nonyloxy)phenyl)methanol, 1-(bromomethyl)-4-(nonyloxy)benzene were resynthesized and characterized as described previously by Wisastra et al. [37].

4.1.2. Synthetic procedure 1: Williamson ether synthesis

Substituted benzyl alcohol (1.0 mmol) and K_2CO_3 (3.0 mmol) were dissolved in DMF (10 mL). Then, 1-bromo alkane (1.1 mmol) was added and the suspension was stirred overnight at room temperature. The reaction mixture was diluted with ethyl acetate (15 mL) and washed with water (3 × 20 mL) and brine (2 × 20 mL). The organic layers were dried over $MgSO_4$, filtered and the solvent was evaporated under reduce pressure.

4.1.3. Synthetic procedure 2: reduction of the aldehyde

$NaBH_4$ (1.1 mmol) was added to the alkoxy benzyl aldehyde (1.0 mmol) in methanol (5.0 mL) under nitrogen atmosphere. The reaction was stirred for 1 h at room temperature. The reaction mixture was concentrated under reduced pressure and water

Table 3
Enzyme kinetic parameters for inhibition of h-15-LOX-1 by **8a** (PK147).

8a (PK147) (μM)	K_m^{app} (μM)	V_{max}^{app} (absorbance/s)	*P-value*
0	8.17 ± 4.9	$7.4 \times 10^{-4} \pm 3.1 \times 10^{-4}$	0.040
10	14.9 ± 5.0	$7.7 \times 10^{-4} \pm 2.3 \times 10^{-4}$	0.012
20	18.9 ± 14	$4.7 \times 10^{-4} \pm 3.6 \times 10^{-4}$	0.022

All the p-values were calculated in GraphPad Prism after linear regression fit. The p-values show that the slopes are significantly non-zero (p-value < 0.05).

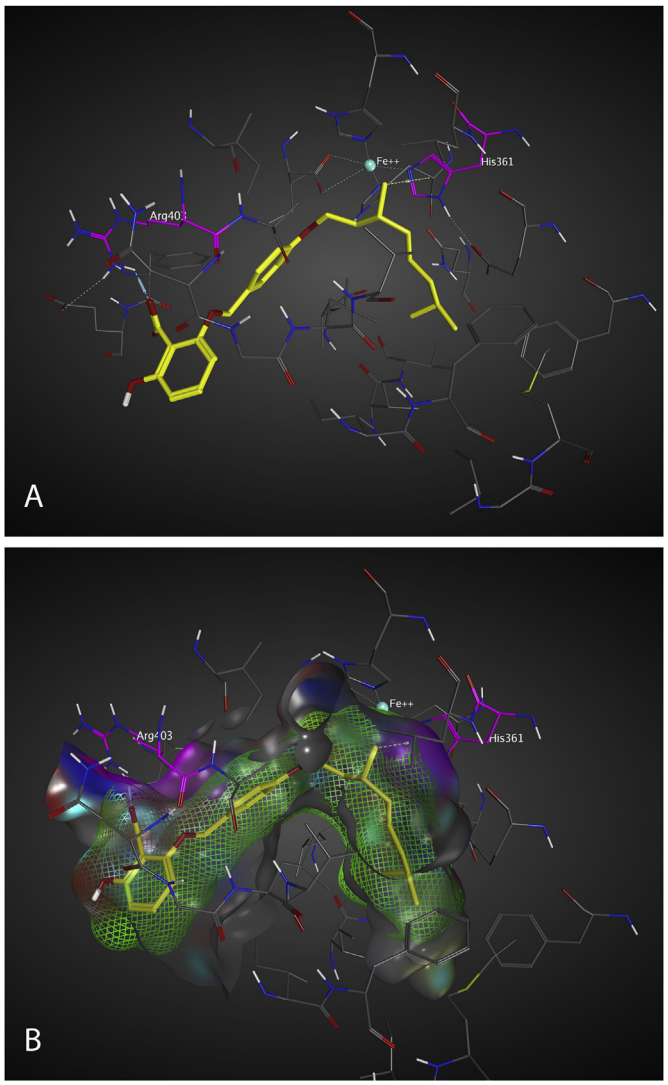

Fig. 5. A) The interaction of the compound **37a** with the active site of the enzyme, B) the surface of the active site of the enzyme and the lipophilic surface, with green lines, of the compound **37a**.

Table 4
Comparison of h-15-LOX-1 inhibition values with docking scores in the enzyme active site.

Compound	IC_{50} (μM)	Score
8b	≈50	−5.44
8c	>50	−4.73
8d	>50	−4.86
37a	7.1 ± 4.6	−6.93
37b	42 ± 12	−5.49
20	>50	−4.24
21	>50	−3.37
22	>50	−4.81
23	>50	−4.68
24	>50	−4.13
25	>50	−4.44
26	>50	−4.62
27	>50	−4.67
28	≈50	−5.65
29	≈50	−5.22

Table 5
Binding affinity of the inhibitor **37a** (N206) for h-15-LOX-1 and ligand efficiency metrics.

Name	Calculated values	Reference values [47,48]
K_i (μM)	1.7	–
LE	0.27	>0.3
BEI	14.4	25.8 ± 7.9
SEI	7.3	14.5 ± 8.7

(20 mL) was added. The mixture was extracted with ethyl acetate (3 × 20 mL). The combined organic layers were dried with $MgSO_4$, filtered and the solvent was evaporated under reduced pressure.

4.1.4. Synthetic procedure 3: bromination of the alkoxy benzyl alcohol

Alkoxy benzyl alcohol (2.0 mmol) was dissolved in DCM (5.0 mL)under nitrogen atmosphere at 0 °C. After 3 min phosphorus tribromide (1.0 mmol) was added dropwise and then the solution was stirred for 2 h at 0 °C. Subsequently, water (20 mL) was added and the mixture was extracted with dichloromethane (3 × 20 mL). The combined organic layers were dried with $MgSO_4$, filtered and the solvent was removed under reduced pressure.

4.1.5. Synthetic procedure 4: protection of 2–6, dyhydrobenzoic acid with acetone

2-6, dihydroxybenzoic acid (1.0 mmol) and DMAP (0.050 mmol) were dissolved in DME (10 mL) under nitrogen atmosphere at 0 °C. Acetone (1.3 mmol) and thionyl chloride (1.3 mmol) were subsequently added dropwise each over 5 min. The solution was stirred at 0 °C for 1 h, then at room temperature for 24 h. An aqueous saturated $NaHCO_3$ (30 mL) was added slowly. 1 N HCl (60 mL) was added and extracted with ethyl acetate (3 × 100 mL). The combined organic layers were dried with $MgSO_4$, filtered and the solvent was removed under reduced pressure. The product was purified by column chromatography.

4.1.6. Synthetic procedure 5: deprotection of the acetonide

The acetonide product (1.0 mmol) was dissolved in THF (10 mL). An aqueous solution of 5 M KOH (2.0 mmol, 0.40 mL) was added and the reaction was heated to 60 °C and stirred for 24 h. THF was removed under reduced pressure and the product was obtained as potassium salt.

4.1.7. Synthetic procedure 6: reduction of the alkene

The alkene (1.0 mmol) and Pd/C (10%) (0.10 mmol) were suspended in EtOH (10 mL). The suspension was stirred under H_2 atmosphere at 40 °C overnight. Subsequently, the mixture was filtered through Celite and after that, the solvent was evaporated under reduce pressure.

4.1.8. Synthetic procedure 7: bromination of aliphatic alcohols

Tetrabromomethane (1.1 mmol) and triphenylphosphine (1.2 mmol) were dissolved in DCM (5.0 mL). The solution was cooled down to 0 °C and the alcohol (1.0 mmol) was added. The solution was stirred for 3 h at 0 °C. Subsequently, petroleum ether (30 mL) was added to precipitate the side product phosphine oxide. After filtration, the organic layer was washed with water (30 mL) and brine (30 mL). The combined organic layers were dried over $MgSO_4$, filtered and concentrated under reduce pressure. The product was purified using column chromatography with petroleum ether:EtOAc 20:1 (v/v) as eluent.

4.1.9. (4-propoxyphenyl)methanol

The product was obtained by coupling of bromopropane and 4-hydroxybenzaldehyde using synthetic procedure 1 followed by aldehyde reduction using synthetic procedure 2. The product was used for the next reaction step without further purification. Colourless to white crystal, yield 87%. ^{1}H NMR (500 MHz, $CDCl_3$) δ 7.24 (d, J = 8.6 Hz, 2H), 6.87 (d, J = 8.6 Hz, 2H), 4.57 (s, 2H), 3.90 (t, J = 6.5, 2H), 2.02 (s, 1H), 1.83–1.76 (m, 2H), 1.03 (t, J = 7.3, 3H). ^{13}C NMR (126 MHz, $CDCl_3$) δ 158.4, 132.9, 128.4, 114.3, 69.3, 64.4, 22.4, 10.3. MS (ESI): m/z 149.4 $[M - H_2O]^{+\cdot}$

4.1.10. 1-(bromomethyl)-4-propoxybenzene

The product was obtained from (4-propoxyphenyl)methanol using synthetic procedure 3. The product was obtained in high purity and no further purification was required. Yellow oil, yield quantitative. ^{1}H NMR (500 MHz, $CDCl_3$) δ 7.28 (d, J = 8.6 Hz, 2H), 6.85 (d, J = 8.6 Hz, 2H), 4.48 (s, 2H), 3.90 (t, J = 6.5, 2H), 1.83–1.75 (m, 2H), 1.02 (t, J = 7.5, 3H). ^{13}C NMR (126 MHz, $CDCl_3$) δ 159.2, 130.3, 129.6, 114.6, 69.4, 34.0, 22.5, 10.4. MS (ESI): m/z 149.1 $[M - Br]^{+\cdot}$

*4.1.11. Potassium 2-hydroxy-6-((4-propoxybenzyl)oxy)benzoate (**8d**, TBK10)*

1-(bromomethyl)-4-propoxybenzene was coupled to 5-hydroxy-2,2-dimethyl-4H-benzo[d][1,3]dioxin-4-one using synthetic procedure 1. The final product was obtained after deprotection according to synthetic procedure 5. Brown solid, yield 68%. Decomposed above 200 °C. ^{1}H NMR (500 MHz, MeOD) δ 7.44 (d, J = 7.8 Hz, 2H), 7.10 (t, J = 8.2 Hz, 1H), 6.90 (d, J = 7.8 Hz, 2H), 6.45 (m, 2H), 5.08 (s, 2H), 3.94 (t, J = 6.3 Hz, 2H), 1.92 (s, 1H), 1.85–1.75 (m, 2H), 1.06 (t, J = 7.4 Hz, 3H) ^{13}C NMR (126 MHz, MeOD) δ 191.3, 175.6, 162.2, 161.1, 133.5, 132.2, 130.9, 116.4, 111.5, 106.9, 99.9, 72.7, 71.6, 24.8, 11.9. MS (ESI): m/z 301.1 $[M]^+$. Elemental analysis for $[C_{17}H_{17}KO_5 + K^+ + OH^-]$: found C: 51.47, H: 4.61 and calculated C: 51.49, H: 4.58.

*4.1.12. 1-chloro-4-((4-((3,7-dimethyloctyl)oxy)benzyl)oxy)benzene (**17**, TBK25)*

1-(bromomethyl)-4-((3,7-dimethyloctyl)oxy)benzene was coupled to 4-chlorophenol using synthetic procedure 1 to obtain the final product. The product washed with methanol. Yellow solid, yield 30%. mp 63–65 °C. ^{1}H NMR (500 MHz, $CDCl_3$) δ 7.32 (d, J = 8.5 Hz, 2H), 7.23 (d, J = 8.9 Hz, 2H), 6.90 (m, 4H), 4.95 (s, 2H), 4.07–3.92 (m, 2H), 1.83–1.81 (m, 1H), 1.61–1.52 (m, 3H), 1.34–1.30 (m, 3H), 1.18–1.15 (m, 3H), 0.97–0.84 (m, 9H). ^{13}C NMR (126 MHz, $CDCl_3$) δ 159.3, 157.6, 129.5, 129.4, 128.5, 125.9, 116.4, 114.8, 70.3, 66.6, 39.4, 37.5, 36.4, 30.0, 28.1, 24.8, 22.9, 22.8, 19.8. MS (ESI): m/z 373.3 $[M]^{+\cdot}$. Elemental analysis for $[C_{23}H_{31}ClO_2]$: found C: 73.61, H: 8.35 and calculated C: 73.68, H: 8.33.

*4.1.13. 4-((4-((3,7-dimethyloctyl)oxy)benzyl)oxy)-1H-indole (**18**, N78)*

1-(bromomethyl)-4-((3,7-dimethyloctyl)oxy)benzene was coupled to 1H-indol-4-ol using synthetic procedure 1 to obtain the final product. The product was purified using column chromatography with heptane:EtOAc 10:1 (v/v) as eluent. Orange oil, yield 50%. ^{1}H NMR (500 MHz, $CDCl_3$) δ 8.04 (s, 1H), 7.36 (d, J = 8.3 Hz, 2H), 7.23–7.18 (m, 2H), 7.12–7.11 (m, 1H), 6.93–6.89 (m, 3H), 6.45 (s, 1H), 5.01 (s, 2H), 4.05–3.95 (m, 2H), 1.84–1.80 (m, 1H), 1.54–1.50 (m, 3H), 1.34–1.26 (m, 3H), 1.18–1.14 (m, 3H), 0.94–0.93 (m, 3H), 0.88–0.87 (m, H). ^{13}C NMR (126 MHz, $CDCl_3$) δ 158.8, 153.4, 131.1, 129.2, 128.2, 124.9, 114.5, 113.1, 111.6, 104.0, 103.4, 102.3, 70.7, 66.3, 39.2, 37.3, 36.2, 29.8, 27.9, 24.6, 22.7, 22.6, 19.6. MS (ESI): m/z 378.3 $[M]^+$.

*4.1.14. 1-(4-((4-((3,7-dimethyloctyl)oxy)benzyl)oxy)phenyl) propan-1-one (**19**, N193)*

1-(bromomethyl)-4-((3,7-dimethyloctyl)oxy)benzene was coupled to 1-(4-hydroxyphenyl)propan-1-one using synthetic procedure 1 to obtain the final product. Yellow solid, yield 70%. mp 70–72 °C. ^{1}H NMR (500 MHz, $CDCl_3$) δ 7.93 (d, J = 8.6 Hz, 2H), 7.33 (d, J = 8.5 Hz, 2H), 6.99 (d, J = 8.6 Hz, 2H), 6.92 (d, J = 8.5 Hz, 2H), 5.04 (s, 2H), 4.04–3.96 (m, 2H), 2.96 (q, J = 7.5 Hz, 2H), 1.86–1.79 (m, 1H), 1.62–1.50 (m, 3H), 1.34–1.26 (m, 3H), 1.18–1.14 (m, 3H), 0.95–0.86 (m, 9H). ^{13}C NMR (126 MHz, $CDCl_3$) δ 199.5, 162.5, 159.2, 130.2, 129.3, 127.9, 114.7, 114.5, 100.0, 70.0, 66.4, 39.2, 37.3, 36.1, 31.4, 29.8, 28.0, 24.6, 22.7, 22.6, 19.6, 8.4. MS (ESI): m/z 419.3 $[M + Na]^{+\cdot}$. Elemental analysis for $[C_{26}H_{36}O_3]$: found C: 78.72, H: 9.18 and calculated C: 78.75, H: 9.15.

*4.1.15. 1-chloro-4-((4-propoxybenzyl)oxy)benzene (**20**, TBK29)*

1-(bromomethyl)-4-propoxybenzene was coupled to 4-chlorophenol using synthetic procedure 1 to obtain the final product. White solid, yield 20%. mp 89–91 °C. ^{1}H NMR (500 MHz, $CDCl_3$) δ 7.32 (d, J = 8.5 Hz, 2H), 7.23 (d, J = 8.9 Hz, 2H), 6.90 (m, 4H), 4.95 (s, 2H), 3.93 (t, J = 6.6 Hz, 2H), 1.86–1.77 (m, 2H), 1.04 (t, J = 7.4 Hz, 3H). ^{13}C NMR (126 MHz, $CDCl_3$) δ 159.3, 157.6, 129.5, 129.4, 128.5, 125.9, 116.4, 114.8, 70.3, 69.8, 22.7, 10.7. MS (ESI): m/z 275.1 $[M]^{+\cdot}$. Elemental analysis for $[C_{16}H_{17}ClO_2]$: found C: 69.56, H: 6.26 and calculated C: 69.44, H: 6.19.

*4.1.16. 1-(4-((4-propoxybenzyl)oxy)phenyl)propan-1-one (**21**, B10)*

1-(bromomethyl)-4-propoxybenzene was coupled to 1-(4-hydroxyphenyl)propan-1-one using synthetic procedure 1 to obtain the final product. Yellow solid, yield 90%. mp 87–89 °C. ^{1}H NMR (500 MHz, $CDCl_3$) δ 7.95 (d, J = 8.8 Hz, 2H), 7.37 (d, J = 8.5 Hz, 2H), 7.04 (d, J = 8.8 Hz, 2H), 6.94 (d, J = 8.5 Hz, 2H), 5.07 (s, 2H), 3.95 (t, J = 6.6 Hz, 2H), 2.96 (m, 2H), 1.85–1.80 (m, 2H), 1.21 (t, J = 7.5 Hz, 3H), 1.06 (t, J = 7.4 Hz, 3H). ^{13}C NMR (126 MHz, $CDCl_3$) δ 198.9, 162.2, 158.7, 134.3, 129.7, 128.9, 114.5, 114.1, 114.1, 69.5, 69.1, 36.0, 30.9, 30.8, 22.1, 10.1, 7.9. MS (ESI): m/z 297.1 $[M]^{+\cdot}$. Elemental analysis for $[C_{19}H_{22}O_3]$: found C: 76.41, H: 7.51 and calculated C: 76.48, H: 7.43.

*4.1.17. 1-nitro-3-((4-propoxybenzyl)oxy)benzene (**22**, B11)*

1-(bromomethyl)-4-propoxybenzene was coupled to 3-nitrophenol using synthetic procedure 1 to obtain the final product. Yellow solid, yield 95%. mp 72–74 °C. ^{1}H NMR (500 MHz, $CDCl_3$) δ 7.83 (m, 2H), 7.44 (t, J = 8.7 Hz, 1H), 7.37 (d, J = 8.5 Hz, 2H), 7.31 (d, J = 8.7 Hz, 1H), 6.96 (d, J = 8.5 Hz, 2H), 5.08 (s, 2H), 3.96 (t, J = 6.7 Hz, 2H), 1.87–1.80 (m, 2H), 1.07 (t, J = 7.5 Hz, 3H). ^{13}C NMR (126 MHz, $CDCl_3$) δ 159.3, 134.4, 129.9, 129.9, 129.3, 127.5, 122.0, 115.8, 114.7, 110.5, 109.2, 70.5, 69.6, 22.5, 10.5. MS (ESI): m/z 286.0 $[M]^+$. Elemental analysis for $[C_{16}H_{17}NO_4]$: found C: 66.83, H: 5.98, N: 4.91 and calculated C: 66.89, H: 5.96, N: 4.88.

*4.1.18. 1-chloro-4-((4-(pentyloxy)benzyl)oxy)benzene (**23**, TBK33)*

1-(bromomethyl)-4-(pentyloxy)benzene was coupled to 4-chlorophenol using synthetic procedure 1 to obtain to final product. The product washed with methanol. White solid, yield 46%. mp 88–90 °C. ^{1}H NMR (500 MHz, $CDCl_3$) δ 7.32 (d, J = 8.5 Hz, 2H), 7.23 (d, J = 8.9 Hz, 2H), 6.90 (m, 4H), 4.95 (s, 2H), 3.96 (t, J = 6.6, 2H), 1.82–1.75 (m, 2H), 1.49–1.33 (m, 4H), 0.93 (t, J = 7.1 Hz, 3H). ^{13}C NMR (126 MHz, $CDCl_3$) δ 159.1, 157.4, 129.3, 129.2, 128.3, 125.6, 116.2, 114.6, 70.1, 68.0, 28.9, 28.2, 22.5, 14.0. MS (ESI): m/z 303.0 $[M]^{+\cdot}$. Elemental analysis for $[C_{18}H_{21}ClO_2]$: found C: 70.87, H: 6.98 and calculated C: 70.93, H: 6.94.

*4.1.19. 1-Iodo-4-((4-(pentyloxy)benzyl)oxy)benzene (**24**, TBK47)*

1-(bromomethyl)-4-(pentyloxy)benzene was coupled to 4-iodophenol using synthetic procedure 1 to obtain the final product. The product washed with methanol. Light brown solid, yield 50%. mp 101–103 °C. ^{1}H NMR (500 MHz, $CDCl_3$) δ 7.55 (d, J = 8.9 Hz, 2H), 7.31 (d, J = 8.5 Hz, 2H), 6.90 (d, J = 8.5 Hz, 2H), 6.74 (d, J = 8.9 Hz, 2H), 4.95 (s, 2H), 3.96 (t, J = 6.6 Hz, 2H), 1.83–1.75 (m, 2H), 1.49–1.34 (m, 4H), 0.93 (t, J = 7.1 Hz, 3H). ^{13}C NMR (126 MHz, $CDCl_3$) δ 159.3, 158.9, 138.4, 129.4, 128.4117.5, 114.8, 83.1, 70.1, 68.2, 29.1, 28.4, 22.6, 14.2. MS (ESI): m/z 395.3 $[M]^{+\cdot}$. Elemental analysis for $[C_{18}H_{21}IO_2]$: found C: 54.54, H: 5.33 and calculated C: 54.56, H: 5.34.

*4.1.20. 2-((4-(pentyloxy)benzyl)oxy)naphthalene (**25**, TBK48)*

1-(bromomethyl)-4-(pentyloxy)benzene was coupled to naphthalen-2-ol using synthetic procedure 1 to obtain the final product. The product washed with methanol. White solid, yield 40%. mp 103–105 °C. ^{1}H NMR (500 MHz, $CDCl_3$) δ 7.78–7.72 (m, 3H), 7.45–7.32 (m, 3H), 7.24–7.20 (m, 2H), 6.93 (d, J = 8.5 Hz, 2H), 5.10 (s, 2H), 3.97 (t, J = 6.6 Hz, 2H), 1.84–1.76 (m, 2H), 1.49–1.35 (m, 4H), 0.94 (t, J = 7.1 Hz, 3H). ^{13}C NMR (126 MHz, $CDCl_3$) δ 159.3, 157.0, 134.7, 129.6, 129.5, 129.2, 128.9, 127.8, 127.0, 126.5, 123.8, 119.3, 114.8, 107.3, 70.1, 68.2, 29.1, 28.4, 22.6, 14.2. MS (ESI): m/z 319.4 $[M]^{+\cdot}$. Elemental analysis for $[C_{22}H_{24}O_2]$: found C: 82.49, H: 7.51 and calculated C: 82.46, H: 7.55.

*4.1.21. 4-((4-(pentyloxy)benzyl)oxy)benzaldehyde (**26**, TBK55)*

1-(bromomethyl)-4-(pentyloxy)benzene was coupled to 4-hydroxybenzaldehyde using synthetic procedure 1 to obtain the final product. Brown solid, yield 63%. mp 65–67 °C. ^{1}H NMR (500 MHz, $CDCl_3$) δ 9.88 (s, 1H), 7.83 (d, J = 8.7 Hz, 2H), 7.34 (d, J = 8.5 Hz, 2H), 7.07 (d, J = 8.7 Hz, 2H), 6.92 (d, J = 8.5 Hz, 2H), 5.06 (s, 2H), 3.96 (t, J = 6.6 Hz, 2H), 1.83–1.75 (m, 2H), 1.48–1.34 (m, 4H), 0.93 (t, J = 7.1 Hz, 3H). ^{13}C NMR (126 MHz, $CDCl_3$) δ 190.9, 164.0, 159.5, 134.9, 132.1, 130.4, 130.2, 129.4, 128.8, 127.8, 115.3, 114.9, 70.3, 68.2, 29.1, 29.0, 28.3, 22.6, 14.2. MS (ESI): m/z 297.2 $[M]^{+\cdot}$. Elemental analysis for $[C_{19}H_{22}O_3]$: found C: 76.44, H: 7.45 and calculated C: 76.48, H: 7.43.

*4.1.22. 2-((4-(pentyloxy)benzyl)oxy)benzaldehyde (**27**, TBK57)*

1-(bromomethyl)-4-(pentyloxy)benzene was coupled to 2-hydroxtbenzaldehyde using synthetic procedure 1 to obtain the final product. Brown solid, yield 54%. mp 28–30 °C. ^{1}H NMR (500 MHz, $CDCl_3$) δ 10.55 (s, 1H), 7.87 (dd, J = 7.7, 1.6 Hz, 1H), 7.55 (td, J = 7.7, 1.6 Hz, 1H), 7.37 (d, J = 8.5 Hz, 2H), 7.10–7.04 (m, 2H), 6.94 (d, J = 8.5 Hz, 2H), 5.13 (s, 2H), 3.99 (t, J = 6.6 Hz, 2H), 1.86–1.77 (m, 2H), 1.50–1.38 (m, 4H), 0.96 (t, J = 7.1 Hz, 3H). ^{13}C NMR (126 MHz, $CDCl_3$) δ 190.0, 161.3, 159.4, 136.0, 129.2, 128.5, 127.9, 121.0, 114.8, 113.3, 70.6, 68.2, 29.8, 29.1, 29.0, 29.0, 28.3, 28.3, 22.6, 14.1. MS (ESI): m/z 297.2 $[M]^+$. Elemental analysis for $[C_{19}H_{22}O_3]$: found C: 76.39, H: 7.44 and calculated C: 76.48, H: 7.43.

*4.1.23. 1-(4-((4-(nonyloxy)benzyl)oxy)phenyl)propan-1-one (**28**, B5)*

1-(bromomethyl)-4-(nonyloxy)benzene was coupled to 1-(4-hydroxyphenyl)propan-1-one using synthetic procedure 1 to obtain the final product. White solid, 72%. mp 73–75 °C. ^{1}H NMR (500 MHz, $CDCl_3$) δ 7.96 (d, J = 8.7 Hz, 2H), 7.35 (d, J = 8.5 Hz, 2H), 7.03 (d, J = 8.7 Hz, 2H), 6.95 (d, J = 8.5 Hz, 2H), 5.07 (s, 2H), 3.99 (t, J = 6.5 Hz, 2H), 2.98 (q, J = 7.0 Hz, 2H), 1.83–1.79 (m, 2H), 1.48–1.31 (m, 12H), 1.24 (t, J = 7.3 Hz, 3H), 0.91 (t, J = 6.5 Hz, 3H). ^{13}C NMR (126 MHz, $CDCl_3$) δ 199.5, 162.5, 159.2, 130.2, 129.2, 127.9, 114.6, 114.5, 114.1, 70.0, 68.1, 31.8, 31.4, 29.5, 29.4, 29.2, 26.0, 25.9, 22.6, 14.1, 8.4. MS (ESI): m/z 381.1 $[M]^+$. Elemental analysis for $[C_{25}H_{34}O_3]$: found C: 78.32, H: 8.99 and calculated C: 78.49, H: 8.96.

*4.1.24. 1-nitro-3-((4-(nonyloxy)benzyl)oxy)benzene (**29**, B6)*

1-(bromomethyl)-4-(nonyloxy)benzene was coupled to 3-

nitrophenol using synthetic procedure 1 to obtain the final product. Yellow solid, 62%. mp 52–54 °C. ^{1}H NMR (500 MHz, $CDCl_3$) δ 7.83 (s, 1H), 7.75 (d, J = 8.5 Hz, 1H), 7.44 (t, J = 8.5 Hz, 1H), 7.37 (d, J = 8.6 Hz, 2H), 7.31 (d, J = 8.5 Hz, 1H), 6.96 (d, J = 8.6 Hz, 2H), 5.08 (s, 2H), 4.00 (t, J = 6.5 Hz, 2H), 1.83–1.80 (m, 2H), 1.48–1.29 (m, 12H), 0.92 (t, J = 6.5 Hz, 3H). ^{13}C NMR (126 MHz, $CDCl_3$) δ 159.3, 129.9, 129.3, 127.5, 122.0, 115.8, 115.2, 114.7, 110.5, 109.2, 70.5, 68.1, 31.8, 29.5, 29.4, 29.2, 29.2, 26.0, 22.6, 14.1. MS (ESI): m/z 370.0 $[M]^{+\cdot}$. Elemental analysis for $[C_{22}H_{29}NO_4]$: found C: 70.94, H: 7.86, N: 3.87 and calculated C: 71.13, H: 7.87, N: 3.77.

*4.1.25. (R)- or (S)-3,7-dimethyloct-6-en-1-ol (**31**)*

The product was obtained from (*R*)- or (*S*)-(−)-Citronellal using synthetic procedure 6. The product was obtained in high purity and no further purification was required. Colourless oil, yield quantitative. ^{1}H NMR (500 MHz, $CDCl_3$) δ 5.05 (m, 1H), 3.58 (m, 2H), 1.97–1.90 (m, 2H), 1.63 (s, 3H), 1.54 (s, 3H), 1.53–1.49 (m, 2H), 1.33–1.29 (m, 2H), 1.14–1.11 (m, 1H), 0.86 (d, J = 6.6 Hz, 3H). ^{13}C NMR (126 MHz, $CDCl_3$) δ 130.9, 124.6, 60.6, 39.7, 37.1, 29.1, 25.5, 25.3, 19.4, 17.4.

*4.1.26. (R)- or (S)-3,7-dimethyloctan-1-ol (**32**)*

The product was obtained from (R)- or (S)-3,7-dimethyloct-6-en-1-ol (**31**) using synthetic procedure 2. The product was obtained in high purity and no further purification was required. Colourless oil, yield quantitative. ^{1}H NMR (500 MHz, $CDCl_3$) δ 3.65–3.60 (m, 2H), 2.18 (s, 1H), 1.58–1.48 (m, 2H), 1.36–1.27 (m, 6H), 1.12–1.10 (m, 2H), 0.87–0.83 (m, 9H). ^{13}C NMR (126 MHz, $CDCl_3$) δ 61.0, 39.9, 39.2, 37.3, 29.5, 27.9, 24.6, 22.6, 22.5, 19.6.

*4.1.27. (S)- or (R)-1-bromo-3,7-dimethyloctane (**33**)*

The product was obtained from (R)- or (S)-3,7-dimethyloct-6-en-1-ol (**32**) using synthetic procedure 7. The product was purified using column chromatography with heptane:EtOAc 30:1 (v/v) as eluent. Yellow oil, yield 65%. ^{1}H NMR (500 MHz, $CDCl_3$) δ 3.47–3.36 (m, 2H), 1.89–1.85 (m, 1H),1.68–1.61 (m, 2H), 1.53–1.50 (m, 1H), 1.34–1.27 (m, 3H), 1.16–1.11 (m, 3H), 0.89–0.85 (m, 9H). ^{13}C NMR (126 MHz, $CDCl_3$) δ 40.0, 39.1, 36.7, 32.1, 31.6, 29.7, 27.9, 24.5, 22.6, 18.9.

*4.1.28. (R)- or (S)-(4-((3,7-dimethyloctyl)oxy)phenyl)methanol (**34**)*

The product was obtained using synthetic procedure 1 between (S)- or (R)-1-bromo-3,7-dimethyloctane and 4-hydroxybenzaldehyde using synthetic procedure 1 followed by aldehyde reduction using synthetic procedure 2. The product was used for the next reaction step without further purification. Yellow oil, yield 80%.^{1}H NMR (500 MHz, $CDCl_3$) δ 7.27 (d, J = 8.5 Hz, 2H), 6.91 (d, J = 8.5 Hz, 2H), 4.58 (s, 2H), 4.01 (m, 2H), 2.45 (s, 1H), 1.89–1.82 (m, 1H), 1.73–1.55 (m, 3H), 1.38–1.27 (m, 3H), 1.22–1.18 (m, 3H), 0.99 (d, J = 6.7 Hz, 3H), 0.92 (d, J = 6.7 Hz, 6H). ^{13}C NMR (126 MHz, $CDCl_3$) δ 158.6, 132.9, 128.5, 114.4, 66.3, 64.7, 39.2, 37.2, 36.1, 29.8, 27.9, 24.6, 22.6, 22.5, 19.6.

*4.1.29. (R)- or (S)-1-(bromomethyl)-4-((3,7-dimethyloctyl)oxy) benzene (**35**)*

The product was obtained from (R)- or (S)-(4-((3,7-dimethyloctyl)oxy)phenyl)methanol using synthetic procedure 3. The product was obtained in high purity and no further purification was required. Yellow oil, yield 87%. ^{1}H NMR (500 MHz, $CDCl_3$) δ 7.30 (d, J = 8.5 Hz, 2H), 6.87 (d, J = 8.5 Hz, 2H), 4.51 (s, 2H), 4.00 (m, 2H), 1.86–1.79 (m, 1H), 1.70–1.52 (m, 3H), 1.35–1.28 (m, 3H), 1.19–1.15 (m, 3H), 0.96 (d, J = 6.7 Hz, 3H), 0.89 (d, J = 6.7 Hz, 6H). ^{13}C NMR (126 MHz, $CDCl_3$) δ 159.2, 130.3, 129.6, 114.6, 66.3, 39.1, 37.2, 36.0, 34.0, 29.7, 27.9, 24.6, 22.6, 22.5, 19.5.

*4.1.30. (R)- or (S)-5-((4-((3,7-dimethyloctyl)oxy)benzyl)oxy)-2,2-dimethyl-4H-benzo[d][1,3]dioxin-4-one (**36**)*

(R)- or (S)-1-(bromomethyl)-4-((3,7-dimethyloctyl)oxy)benzene was coupled to 5-hydroxy-2,2-dimethyl-4H-benzo[d][1,3] dioxin-4-one using synthetic procedure 1 to obtain the final product. The product was purified using column chromatography with heptane:EtOAc 20:1 (v/v) as eluent. Yellow solid, yield 68%. ^{1}H NMR (500 MHz, $CDCl_3$) δ 7.43 (d, J = 8.5, 2H), 7.39 (t, J = 8.4, 1H), 6.90 (d, J = 8.5, 2H), 6.66 (d, J = 8.5, 1H), 6.53 (d, J = 8.2, 1H), 5.18 (s, 2H), 3.98 (m, 2H), 1.83–1.79 (m, 1H), 1.70 (s, 6H), 1.57–1.50 (m, 3H), 1.34–1.31 (m, 3H), 1.17–1.14 (m, 3H), 0.94 (d, J = 6.7 Hz, 3H), 0.87 (d, J = 6.7 Hz, 6H). ^{13}C NMR (126 MHz, $CDCl_3$) δ 160.4, 158.8, 158.0, 157.7, 136.2, 128.3, 128.0, 114.6, 109.3, 107.4, 105.2, 70.6, 66.3, 39.2, 37.2, 36.2, 29.8, 29.7, 27.9, 25.6, 24.6, 22.7, 22.6, 19.6.

*4.1.31. Potassium (R)- or (S)-2-((4-((3,7-dimethyloctyl)oxy)benzyl) oxy)-6-hydroxybenzoate (**37a**/**37b**)*

The final product was obtained after deprotection of (R)- or (S)-5-((4-((3,7-dimethyloctyl)oxy)benzyl)oxy)-2,2-dimethyl-4H-benzo[d][1,3]dioxin-4-one (**36**) according to synthetic procedure 5. The product was obtained in high purity and no further purification was required. White solid, yield quantitative. ^{1}H NMR (500 MHz, MeOD) δ 7.38 (d, J = 8.3, 2H), 6.86 (d, J = 8.5, 1H), 6.83 (t, J = 8.0, 2H), 6.30 (d, J = 8.0, 1H), 6.16 (d, J = 8.0, 1H), 4.94 (s, 2H), 3.98 (q, J = 6.4, 2H), 1.80–1.75 (m, 1H), 1.66–1.49 (m, 3H), 1.35–1.26 (m, 3H), 1.18–1.14 (m, 3H), 0.92 (d, J = 6.7 Hz, 3H), 0.87 (d, J = 6.7 Hz, 6H). ^{13}C NMR (126 MHz, MeOD) δ 189.7, 165.2, 160.4, 158.0, 131.6, 130.2, 129.4, 115.4, 114.3, 101.2, 71.6, 67.4, 40.6, 38.6, 37.5, 31.1, 29.3, 26.0, 23.2, 22.4, 20.4. Elemental analysis for **37a** (N206) $[C_{24}H_{31}KO_5 + K^+ + OH^-]$: found C: 58.24, H: 6.51 and calculated C: 58.27, H: 6.52, for **37b** (N219) $[C_{24}H_{31}KO_5 + K^+ + OH^-]$: found C: 58.23, H: 6.54 and calculated C: 58.27, H: 6.52.

4.2. Enzyme activity studies

4.2.1. Expression and purification of His_6-tagged h-15-LOX-1

The h-15-LOX-1-His_6 protein, carrying an N-terminal His6-tag without a linker-sequence, was produced in *E. coli* BL21(DE3) using the T7 expression system. Fresh transformed BL21(DE3) containing the expression plasmid pET26 (15-LOX-1-His_6) were collected from an LB plate and used to inoculate LB medium (5 mL). After growth for 3–6 h at 37 °C, this culture was used to inoculate fresh LB medium (1 L) to a starting OD600 of about 0.01. LB agar plates and LB medium were supplemented with kanamycin (30 μg/mL). After overnight growth at 37 °C, the culture was equilibrated at 26 °C for 1 h after which expression of the 15-LOX-1 gene was induced by the addition of IPTG to a final concentration of 1 mM (from a 1 M stock solution in water). The culture was subsequently incubated at 26 °C for 4 h for protein production. Throughout this procedure, the culture was subjected to vigorous shaking (150 rpm). Subsequently, cells were harvested by centrifugation (10 min at 2300 g) and resuspended in 25 mM HEPES buffer, pH 7.5, (Buffer A) to a total volume of about 10 mL. Protease inhibitors (Complete Mini, Roche, Mannheim, Germany) were added and cells were disrupted by sonication for 1 min at 50% duty cycle/50% output using a Branson Sonifier 450 (Branson Ultrasonics Corporation, Danbury, CT). Unbroken cells and debris were removed by centrifugation (30 min at 15000 g). The supernatant was applied to a gravity flow column containing 0.5 mL Ni-Sepharose 6 Fast Flow resin. The nonbound proteins were removed from the column by gravity flow. The column was washed with 50 mM imidazole in buffer A, after which retained proteins were eluted with 1 mL of 250 mM imidazole in buffer A. Subsequently, the protein sample was applied to a PD-10 gelfiltration column, which was previously equilibrated in 25 mM HEPES buffer, pH 7.5, supplemented with 5%

(v/v) glycerol (buffer B), and proteins were eluted with buffer B. Fractions (1 mL) were analysed by SDS-PAGE, and those containing highly purified 15-LOX were combined and concentrated to a protein concentration of about 10 mg/mL using a Vivaspin centrifugal concentrator equipped with a 30,000 Da molecular weight cut-off filtration membrane (Sartorius Stedim Biotech S.A., France). The purified protein was flash-frozen in liquid nitrogen upon completion of this procedure and stored at −80 °C until further use. The purity of h-15-LOX-1 was assessed by SDS-PAGE (Fig. S1).

4.2.2. Activity assay

For the activity assay, h-15-LOX-1 was expressed in BL21 DE3 cells and the crude lysate was used without further purification. h-15-LOX-1 activity was determined by the conversion of linoleic acid to 13S-hydroperoxy-9Z,11E-octadecadienoic acid (13(S)-HpODE). The conversion rate was followed by UV-absorbance at 234 nm over time. The linear increase in absorbance was used to determine the enzyme activity. The linear part usually covers the first 10–16 min depending on the enzyme concentration after which the conversion rate goes down due to depletion of the substrate. The optimum concentration of h-15-LOX-1 was determined by an enzyme activity assay (x 640 times dilution). Data analysis was done using the Microsoft Excel Professional 2010 and Graphpath Prism 5.01 software.

4.2.3. Human h-15-LOX-1 screening UV assay

The screening UV assay of h-15-LOX-1 was also studied by the formation of 13(S)-HPODE at 234 nm using a similar experimental setup as for the enzyme activity assay. The assay buffer consists of 25 mM HEPES titrated to pH 7.5 using a concentrated aqueous solution of NaOH. The substrate, linoleic acid (LA) (Sigma Aldrich, L1376) was diluted in ethanol to 500 μM. The enzyme was diluted 1:160 with assay buffer. The inhibitor (100 mM in DMSO) was diluted with the assay buffer to 125 μM. The inhibitor solution of 80 μL was mixed with 60 μL assay buffer, 50 μL of 1:160 enzyme solution and incubated for 10 min at RT. After incubation, 10 μL of 500 μM LA was added to the mixture which provided a mixture with a final dilution of the enzyme of 1:640 and 25 μM LA. The linear absorbance increase in absence of the inhibitor was set as 100%, whereas the absorbance increase in absence of the enzyme was set to 0%. All experiments were performed in triplicate and the average triplicate values and their standard deviations are plotted.

The half maximal inhibitor concentration (IC_{50}) of the inhibitors for h-15-LOX-1 was determined using the same assay. The inhibitor was diluted to 250 μM with assay buffer. Subsequently, using a serial dilution, the desired dilutions of the inhibitor were obtained ranging from 0.19 to 100 μM.

4.2.4. Michaelis–Menten enzyme kinetics

In this kinetic study, 25 mM HEPES buffer, pH 7.5, was used as an assay buffer. The enzyme was diluted 1:160 with assay buffer while linoleic acid (Sigma Aldrich, L1376-1G) was diluted with EtOH to 4 mM. LA concentrations ranging from 0.05 to 3 mM were made using the 4 mM LA stock solution. The enzyme activity was measured in the absence or presence of fixed concentrations of the inhibitor (0 μM, 10 μM and 20 μM). 50 μL of the enzyme solution was mixed with 80 μL of inhibitor (25 μM or 50 μM), 60 μL assay buffer and incubated for 10 min at RT. In absence of the inhibitor, the amount of inhibitor is substituted with assay buffer. Subsequently, 10 μL of LA solution ranging from 0.05 to 4 mM was added to the mixture to provide a mixture with a final dilution of the enzyme of 1:640. The mixtures were immediately measured after 5 s of mixing the enzyme with the inhibitor and substrate for 16 min. These experiments were executed in triplicate. The reaction velocities (v) were plotted against the substrate concentrations in a Michaelis–Menten plot and the K_m and V_{max} in the presence of the inhibitor were derived. The reciprocal of the velocities were taken and plotted against the reciprocal of the LA concentrations in a Lineweaver–Burk plot. Substrate inhibition was obtained in concentration above 60 μM. All experiments were performed in triplicate and the average triplicate values and their standard deviations are plotted. The data analysis was performed using Microsoft Excel Professional Plus 2013 and GraphPad Prism 5.01.

Acknowledgements

We acknowledge the Netherlands Organisation for Scientific Research (NWO) for providing a VIDI grant (016.122.302) to F.J.D. We acknowledge T. Holman University of California, Santa Cruz for providing the h-15-LOX-1 plasmid.

Appendix A. Supplementary data

Supplementary data associated with this article can be found in the online version, at http://dx.doi.org/10.1016/j.ejmech.2015.03.007. These data include MOL files and InChiKeys of the most important compounds described in this article.

References

[1] A.P. Kulkarni, Cell. Mol. Life. Sci. 58 (2001) 1805–1825.
[2] A.R. Brash, J. Biol. Chem. 274 (1999) 23679–23682.
[3] A. Andreou, I. Feussner, Phytochemistry 70 (2009) 1504–1510.
[4] J.Z. Haeggström, C.D. Funk, Chem. Rev. 111 (2011) 5866–5898.
[5] K. Okunishi, M. Peters-Golden, Biochim. Biophys. Acta. 1810 (2011) 1096–1102.
[6] B. Samuelsson, S. Dahlen, J.A.N.A. Lindgren, C.A. Rouzer, C.N. Serhan, Science 237 (1987) 1171–1176.
[7] E. Sigal, C.W. Laughton, M.A. Mulkins, Ann. N. Y. Acad. Sci. 714 (1994) 211–224.
[8] Y.-C. Joo, D.-K. Oh, Biotechnol. Adv. 30 (2012) 1524–1532.
[9] R. Wisastra, F.J. Dekker, Cancers (Basel) 6 (2014) 1500–1521.
[10] A.R. Brash, W.E. Boeglin, M.S. Chang, Proc. Natl. Acad. Sci. U. S. A. 94 (1997) 6148–6152.
[11] L.C. Hsi, L.C. Wilson, T.E. Eling, J. Biol. Chem. 277 (2002) 40549–40556.
[12] R.J. Soberman, T.W. Harper, D. Betteridge, R.A. Lewis, K.F. Austen, J. Biol. Chem. 260 (1985) 4508–4515.
[13] D. Klurfeld, A. Bull, Am. J. Clin. Nutr. 66 (1997) 1530S–1538S.
[14] S.M. Earles, J.C. Bronstein, D.L. Winner, A.W. Bull, Biochim. Biophys. Acta 1081 (1991) 174–180.
[15] H.-E. Claesson, Prostaglandins Other Lipid Mediat. 89 (2009) 120–125.
[16] S. Feltenmark, N. Gautam, A. Brunnström, W. Griffiths, L. Backman, C. Edenius, L. Lindbom, M. Björkholm, H.-E. Claesson, Proc. Natl. Acad. Sci. U. S. A. 105 (2008) 680–685.
[17] H. Kühn, V.B. O'Donnell, Prog. Lipid. Res. 45 (2006) 334–356.
[18] H. Kuhn, M. Walther, R.J. Kuban, Prostaglandins Other Lipid Mediat. 68–69 (2002) 263–290.
[19] J. Turk, R. Maas, A. Brash, L. Roberts, J. Biol. Chem. 257 (1982) 7068–7076.
[20] J.A. Hunter, W.E. Finkbeiner, J.A. Nadel, E.J. Goetzl, M.J. Holtzman, Proc. Natl. Acad. Sci. U. S. A. 82 (1985) 4633–4637.
[21] M. Gullikkson, A. Brunnström, M. Johannesson, L. Backman, G. Nilsson, I. Harvima, B. Dahlén, M. Kumlin, H.E. Claesson, Biochim. Biophys. Acta Mol. Cell. Biol. Lipids 1771 (2007) 1156–1165.
[22] D.J. Conrad, H. Kuhn, M. Mulkins, E. Highland, E. Sigal, Proc. Natl. Acad. Sci. U. S. A. 89 (1992) 217–221.
[23] R. Brinckmann, M.S. Topp, I. Zalán, D. Heydeck, P. Ludwig, H. Kühn, W.E. Berdel, J.R. Habenicht, Biochem.. J. 318 (Pt1) (1996) 305–312.
[24] W. Jubiz, O. Rådmark, J. Lindgren, C. Malmsten, B. Samuelsson, Biochem. Biophys. Res. Commun. 99 (1981) 976–986.
[25] R. Maas, A. Brash, Proc. Natl. Acad. Sci. U. S. A. 80 (1983) 2884–2888.
[26] M. Hamberg, J.A.N. Svensson, B. Samuelsson, Proc. Natl. Acad. Sci. U. S. A. 71 (1974) 3824–3828.
[27] M. Kanehisa, S. Goto, Y. Sato, M. Kawashima, M. Furumichi, M. Tanabe, Nucleic Acids Res. 42 (2014) D199–D205.
[28] S.V.K. Mahipal, J. Subhashini, M.C. Reddy, M.M. Reddy, K. Anilkumar, K.R. Roy, G. V Reddy, P. Reddanna, Biochem. Pharmacol. 74 (2007) 202–214.
[29] C. Sachs-Olsen, M. Sanak, A.M. Lang, A. Gielicz, P. Mowinckel, K.C. Lødrup Carlsen, K.-H. Carlsen, A. Szczeklik, J. Allergy Clin. Immunol. 126 (2010), 859–867.e9.
[30] S.M. Sendobry, J.A. Cornicelli, K. Welch, T. Bocan, B. Tait, B.K. Trivedi, N. Colbry, R.D. Dyer, S.J. Feinmark, A. Daugherty, Br. J. Pharmacol. 120 (1997) 1199–1206.

[31] D.S. Weinstein, W. Liu, Z. Gu, C. Langevine, K. Ngu, L. Fadnis, D.W. Combs, D. Sitkoff, S. Ahmad, S. Zhuang, et al., Bioorg. Med. Chem. Lett. 15 (2005) 1435–1440.
[32] D.S. Weinstein, W. Liu, K. Ngu, C. Langevine, D.W. Combs, S. Zhuang, C. Chen, C.S. Madsen, T.W. Harper, J.A. Robl, Bioorg. Med. Chem. Lett. 17 (2007) 5115–5120.
[33] K. Ngu, D.S. Weinstein, W. Liu, C. Langevine, D.W. Combs, S. Zhuang, X. Chen, C.S. Madsen, T.W. Harper, S. Ahmad, et al., Bioorg. Med. Chem. Lett. 21 (2011) 4141–4145.
[34] G. Rai, N. Joshi, J.E. Jung, Y. Liu, L. Schultz, A. Yasgar, S. Perry, G. Diaz, Q. Zhang, V. Kenyon, A. Jadhav, A. Simeonov, E.H. Lo, K. van Leyen, D.J. Maloney, T.R. Holman, J. Med. Chem. 57 (2014) 4035–4048.
[35] M. Mahdavi, M.S. Shirazi, R. Taherkhani, M. Saeedi, E. Alipour, F.H. Moghadam, A. Moradi, H. Nadri, S. Emami, L. Firoozpour, A. Shafiee, A. Foroumadi, Eur. J. Med. Chem. 82C (2014) 308–313.
[36] T. Asghari, M. Bakavoli, M. Rahimizadeh, H. Eshghi, S. Saberi, A. Karimian, F. Hadizadeh, M. Ghandadi, Chem. Biol. Drug Des. (2014), http://dx.doi.org/10.1111/cbdd.12375.
[37] R. Wisastra, P.A.M. Kok, N. Eleftheriadis, M.P. Baumgartner, C.J. Camacho, H.J. Haisma, F.J. Dekker, Bioorg. Med. Chem. 21 (2013) 7763–7778.
[38] R. Wisastra, M. Ghizzoni, A. Boltjes, H.J. Haisma, F.J. Dekker, Bioorg. Med. Chem. 20 (2012) 5027–5032.
[39] M. Uchiyama, H. Ozawa, K. Takuma, Y. Matsumoto, M. Yonehara, K. Hiroya, T. Sakamoto, Org. Lett. 8 (2006) 5517–5520.
[40] M. Ghizzoni, A. Boltjes, C. de Graaf, H.J. Haisma, F.J. Dekker, Bioorg. Med. Chem. 18 (2010) 5826–5834.
[41] T. Amagata, S. Whitman, J. Nat. (2003) 230–235.
[42] T.M.A. Bocan, W.S. Rosebury, S.B. Mueller, Susan Kuchera, K. Welch, A. Daugherty, J.A. Cornicelli, Atherosclerosis 136 (1998) 203–216.
[43] D.S. Weinstein, W. Liu, Z. Gu, C. Langevine, K. Ngu, L. Fadnis, D.W. Combs, D. Sitkoff, S. Ahmad, S. Zhuang, X. Chen, F.L. Wang, D.A. Loughney, K.S. Atwal, R. Zahler, J.E. Macor, C.S. Madsen, N. Murugesan, Bioorg. Med. Chem. Lett. 15 (2005) 1435–1440.
[44] S. Deng, A.K. Palu, B.J. West, C.X. Su, B.N. Zhou, J.C. Jensen, J. Nat. Prod. 70 (2007) 859–862.
[45] S.A. Gillmor, A. Villaseñor, R. Fletterick, E. Sigal, M.F. Browner, Nat. Struct. Biol. 4 (1997) 1003–1009.
[46] I.D. Kuntz, K. Chen, K.A. Sharp, P.A. Kollman, Proc. Natl. Acad. Sci. U. S. A. 96 (1999) 9997–10002.
[47] C. Abad-Zapatero, Expert Opin. Drug Discov. 2 (2007) 469–488.
[48] C. Abad-Zapatero, J. Metz, Drug Discov. Today (2005) 10.